Environmental Science & Technology

pubs.acs.org/est

Article

Development of a Physiologically Based Pharmacokinetic (PBPK) Model for F-53B in Pregnant Mice and Its Extrapolation to Humans

Jing Zhang, Shen-Pan Li, Qing-Qing Li, Yun-Ting Zhang, Guang-Hui Dong, Alexa Canchola, Xiaowen Zeng,* and Wei-Chun Chou*

Cite This: *Environ. Sci. Technol.* 2024, 58, 18928−18939

Read Online

ACCESS | Metrics & More | Article Recommendations | Supporting Information

ABSTRACT: Chlorinated polyfluorinated ether sulfonic acid (F-53B), a commonly utilized alternative for perfluorooctane sulfonate, was detected in pregnant women and cord blood recently. However, the lack of detailed toxicokinetic information poses a significant challenge in assessing the human risk assessment for F-53B exposure. Our study aimed to develop a physiologically based pharmacokinetic (PBPK) model for pregnant mice, based on toxicokinetic experiments, and extrapolating it to humans. Pregnant mice were administered 80 μg/kg F-53B orally and intravenously on gestational day 13. F-53B concentrations in biological samples were analyzed via ultraperformance liquid chromatography−mass spectrometry. Results showed the highest F-53B accumulation in the brain, followed by the placenta, amniotic fluid, and liver in fetal mice. These toxicokinetic data were applied to F-53B PBPK model development and evaluation, and Monte Carlo simulations were used to characterize the variability and uncertainty in the human population. Most of the predictive values were within a 2-fold range of experimental data (>72%) and had a coefficient of determination (R^2) greater than 0.68. The developed mouse model was then extrapolated to the human and evaluated with human biomonitoring data. Our study provides an important step toward improving the understanding of toxicokinetics of F-53B and enhancing the quantitative risk assessments in sensitive populations, particularly in pregnant women and fetuses.

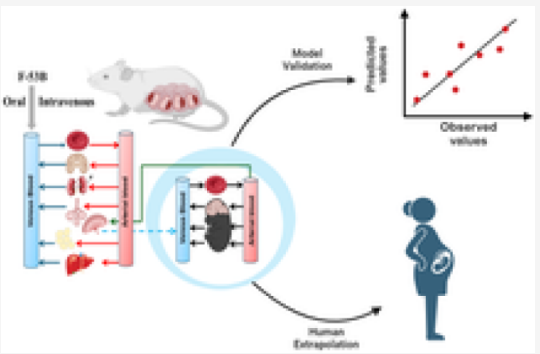

KEYWORDS: *F-53B, physiologically based pharmacokinetic (PBPK) modeling, Monte Carlo (MC) simulation, perfluorooctanesulfonate (PFOS)*

1. INTRODUCTION

Chlorinated polyfluorinated ether sulfonic acid (F-53B), a mixture of mostly 6:2 and 8:2 Cl-PFESAs, was first synthesized in 1970 and was subsequently used widely as a mist suppressant in Chinese industries.[1] With global restrictions on perfluorooctanesulfonate (PFOS), F-53B has emerged as the primary alternative, leading to substantial market expansion in China. However, concerns regarding its environmental presence and potential toxicity have garnered considerable attention.[1] F-53B is widely distributed in various environmental matrices, including air,[2,3] surface water,[4,5] and sediments.[6] Several epidemiological studies have indicated that F-53B can be detected in hair, urine, and nail samples.[7] Additionally, due to its potential trans-placental effect, F-53B has been detected in maternal and cord blood, breast milk, and placenta.[8,9−11] Regarding the potential toxicities of F-53B, limited toxicological studies indicated that F-53B might contribute to hepatic toxicity,[12] reproductive toxicity,[13] development toxicity,[14] and gut microbiota dysbiosis.[12] Despite these emerging health concerns, the lack of regulation of F-53B has led to its continued widespread use.

Early life represents a critical period of susceptibility to exogenous chemical exposure.[15,16,17] Several epidemiological studies have indicated that F-53B can penetrate the placental barrier[8,18] and might be associated with a range of adverse birth outcomes in human populations, including preeclampsia,[19] gestational diabetes mellitus,[20,21] fetal birth weight reduction and increased preterm delivery risk,[11,22] endocrine hormone changes,[23-25] and childhood neurodevelopmental deficiencies.[26] These effects may have detrimental consequences on the offspring's growth and development. Despite the documented potential toxicities, regulating the use of F-53B and characterizing their potential risks is difficult. This is primarily due to lack of detailed toxicokinetic (TK) information necessary for understanding the absorption, distribution, metabolism, and elimination (ADME) properties

Received: June 1, 2024
Revised: September 28, 2024
Accepted: September 30, 2024
Published: October 12, 2024

Table 1. Summary of Experimental Data from Pregnant Mice used in the PBPK Model[a]

	Oral	IV	
Sample size[b]	Measured time (h)	Measured time (h)	Purpose
Plasma (n = 4−6)[c]	2, 4, 8, 12, 24, 36, 48, 72, 96	0.5, 2, 4, 8, 12, 24, 48, 72, 96	Calibration
Liver (n = 2−4)[d]	2, 4, 8, 12, 24, 48, 96	2, 4, 8, 12, 24, 48, 96	Calibration
Fetal brain (n = 2−4)[d]	2, 4, 8, 12, 24, 48, 96	2, 4, 8, 12, 24, 48, 96	Calibration
Fetal liver (n = 2−4)[d]	2, 4, 8, 12, 24, 48, 96	2, 4, 8, 12, 24, 48, 96	Evaluation
Placenta (n = 2−4)[d]	2, 4, 8, 12, 24, 48, 96	2, 4, 8, 12, 24, 48, 96	TK study
Amniotic fluid (n = 4)	96	96	Evaluation
Fat (n = 4)	96	96	Evaluation
Brain (n = 4)[e]	96	96	Evaluation
Heart (n = 4)[e]	96	96	Evaluation
Spleen (n = 4)[e]	96	96	Evaluation
Kidney (n = 4)	96	96	TK study
Small intestine (n = 4)	96	96	TK study
Stomach (n = 4)	96	96	TK study
Urine (n = 4)[f]	0, 0−2, 2−4, 4−8, 8−12, 12−24, 24−36, 36−48, 48−72, 72−96	0, 0−2, 2−4, 4−8, 8−12, 12−24, 24−36, 36−48, 48−72, 72−96	TK study
Feces (n = 4)[f]	0, 0−2, 2−4, 4−8, 8−12, 12−24, 24−36, 36−48, 48−72, 72−96	0, 0−2, 2−4, 4−8, 8−12, 12−24, 24−36, 36−48, 48−72, 72−96	TK study

[a]PBPK, physiologically based pharmacokinetic. Measured time refers to the time after exposure, i.e., 0 h refers to the beginning of GD13; "TK study" refers to data only used to calculate the accumulation. [b]For each time point. [c]Obtained plasma from the repeat blood collection group (n = 4) at each time point and additionally obtained plasma from euthanasia group (n = 2) at time points of 2, 4, 8, 12, 24, and 48 h. [d]At 96 h, four were euthanized and at the remaining time points, two were euthanized. [e]The mean value of the concentrations in these three tissues was taken as the concentration of the rest of the body. [f]Collected from the repeat blood collection group.

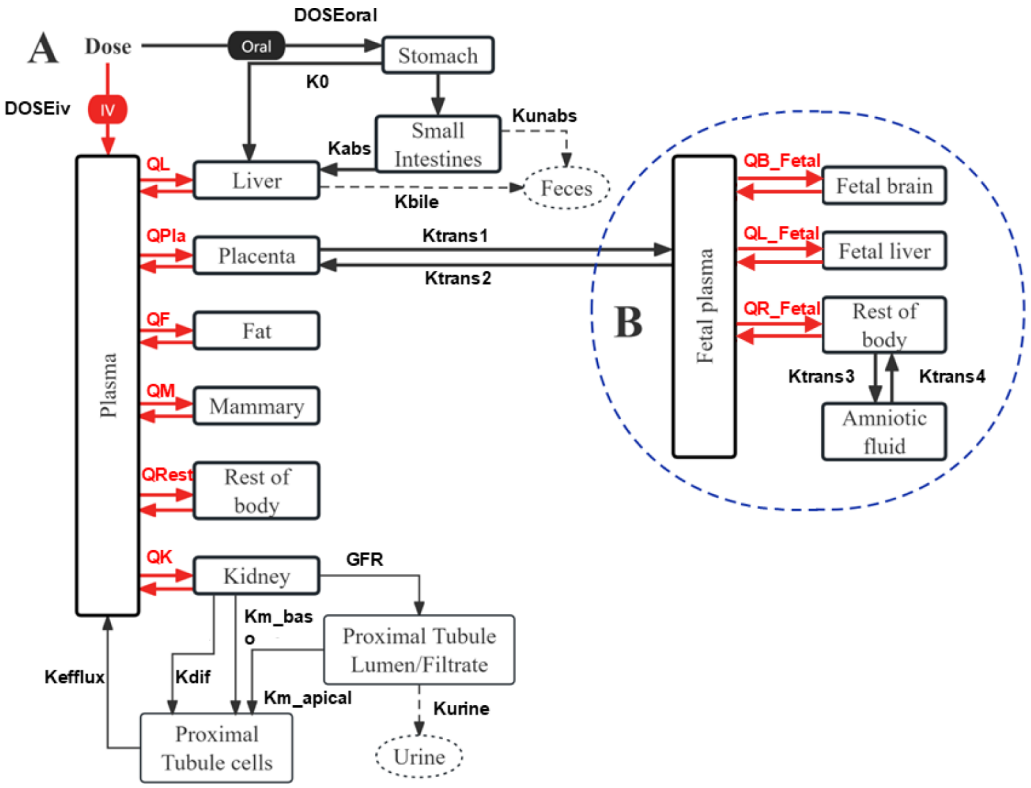

Figure 1. A schematic of the PBPK model for F-53B in pregnant mice and humans. (A) The maternal model consisted of seven compartments, including the plasma, liver, placenta, fat, mammary glands, kidney, and rest of the body. (B) The fetal model consists of the plasma, brain, liver, rest of the body, and amniotic fluid.

of F-53B. Furthermore, a mechanistic model for extrapolating the dosimetry from animal to human populations, as well as accounts of TK variability between species and across life stages, are crucial components of comprehensive risk assessment strategies for PFAS compounds.[27] This gap can be addressed by developing a physiologically based pharmacokinetic (PBPK) model validated across species and life stages.

Previously, our laboratory successfully developed a generic PBPK model for PFOS within a Bayesian framework, applicable to multiple species including mice, rats, monkeys, and humans.[28] Subsequently, this model was extended to

https://doi.org/10.1021/acs.est.4c05405
Environ. Sci. Technol. 2024, 58, 18928−18939

include additional life stages, such as gestation and lactation.[29] Building upon our previous modeling efforts and considering scientific data gaps, the aim of this study was to construct a PBPK model for F-53B specifically for pregnant mice and humans. This model aims to support risk assessment efforts focused on sensitive subpopulations, notably pregnant women and fetuses. Utilizing in-house experimental data from single-dose experiments involving pregnant C57BL/6J female mice administered F-53B orally and intravenously (IV), allows us to calibrate and validate the PBPK model for F-53B in pregnant mice. Monte Carlo (MC) simulations were incorporated into the model to simulate population by characterizing the uncertainty and variability of model parameters on F-53B dosimetry during pregnancy. Subsequently, this model was further extrapolated to human populations and validated with human biomonitoring data collected from the literature. All model code and raw data are openly available on GitHub (https://github.com/choulab210) to support the replication of our findings and allow the application and extension of this model to other PFAS compounds.

2. MATERIALS AND METHODS

2.1. Chemical and Materials. F-53B (CAS: 73606-19-6) was purchased from Jianglaibio Co., Ltd. (Shanghai, China), with a purity of >97%. Chemicals were dissolved in dimethyl sulfoxide (DMSO) to create concentrated stock solutions. All the chemicals used were of HPLC grade or highest quality available; a complete description of target analytes and reagents is given in Tables S1 and S2.

2.2. Toxicokinetic Study in Pregnant Mice. Eighty C57BL/6J female and male mice were obtained from the Medical Laboratory Animal Center of Guangdong, mated in a 1:1 ratio, and maintained under a 12 h light/dark cycle with ad libitum access to food and water. The study was approved by the ethics committee of Sun Yat-Sen University (SYSU-IACUC-2022-001602). The pregnant mice were divided into two groups and administered 80 μg/kg body weight (BW) of F-53B orally (n = 20) or via lateral tail vein injection (n = 20) on gestation day (GD) 13. Dose setting can be found Section S1. Samples of plasma, liver, placenta, urine, and feces were collected from dams, and samples of brain and liver were collected from fetuses from GD13 to GD17, with additional samples of amniotic fluid, fat, brain, heart, spleen, kidney, small intestine, and stomach taken at GD17. Blood samples were taken at specified intervals, and urine and fecal samples were collected regularly (Table 1). Samples were frozen at −80 °C before analysis, with the F-53B content measured using ultraperformance liquid chromatography and protein binding assays conducted by ultrafiltration centrifugation. Detailed treatment and calculations of protein binding methods are described in Sections S2−S3 and eqs S1−S2.

2.3. Development and Validation of the PBPK Model in Pregnant Mice. A PBPK model for pregnant mice (Figure 1) was developed to predict the time-course toxicokinetic profiles of F-53B. The developed PFOS PBPK models during adulthood and pregnancy in rats and humans from our previous studies[28,29] were used as the basis to extrapolate to the present model. Briefly, the pregnancy model structure comprises seven organ compartments, including plasma, liver, kidney, fat, mammary gland, placenta, and other parts of the body. The mouse and human models used a consistent model structure, assuming compartments were homogeneous and interconnected through the circulating blood system (plasma compartment). Both oral and IV exposure routes, based on in-house experimental data, were included in the model. Oral exposure to F-53B was modeled by using a two-compartment system consisting of the stomach and intestines. This system simulates the absorption of F-53B in the stomach followed by its transport to the intestine tract via gastric emptying. (eqs S3−S5). The process of renal reabsorption has been reported to play a critical role in the PFAS fate and biodistribution.[30] Thus, the physiologically based descriptions, including renal reabsorption and basolateral/apical transporters, were included in both mouse and human models (eqs S6−S9). The renal filtration by glomerular filtration rate (GFR) was also incorporated (eqs S10−S11). Elimination of F-53B in the model was described through urine (eq S12) and feces (eq S13). Mass balance differential equations were applied to depict the rate of change of F-53B within each of the compartments defined in the model (eqs S14−S15). However, since the metabolic pathway of F-53B remains poorly understood, metabolisms of F-53B were not considered in our model. Gender-specific physiological parameters, including BW, cardiac output (QCC), the volume of mammary gland and fat, and glomerular filtration rate, were collected from the literature[31−34] and incorporated into the model (Tables S3−S4). The abbreviations of all parameters and their meaning are listed in Table S3.

On the other hand, the fetal submodel included five organ compartments (plasma, fetal brain, fetal liver, rest of the body, and amniotic fluid). The fetal submodel and its circulation were defined as compartments separate from the maternal model. Fetal exposure to F-53B occurs exclusively through placental transfer, with the excretion from the fetal plasma to the placenta, and subsequently returning to maternal circulation (Figure 1). The transfer of F-53B between the placenta and fetal plasma, as well as between the rest of the fetal body and the amniotic fluid compartment, was modeled as a bidirectional diffusion process governed by first-order rate constants (Ktrans1, Ktrans2, Ktrans3, and Ktrans4),[31,35,36] The transfer of F-53B between the placenta and fetus or the rest of the fetal body and the amniotic fluid during pregnancy was defined using eqs S16 − S19.

2.3.1. Model Parameterization and Calibration. The parameters for the pregnancy PBPK model for F-53B in both mice and humans include physiological and chemical-specific parameters. Physiological parameters, such as QCC, fractions of blood flow to specific tissues, BW, and the volume fractions of individual organs, were collected from previous studies[32,34−48] (Table S4). Among these parameters, some parameters, such as BW, QCC, volume of the mammary gland, fat (VF), placenta (VPla), and blood flow of mammary, etc., were described as growth equations reflecting the dynamic changes function during pregnancy (Figure S1 and Tables S5−S6). Chemical-specific parameters included partition coefficients, rate constants of absorption/elimination, partition coefficients, protein binding parameters, and renal reabsorption parameters. The protein binding, partition coefficients, and absorption/elimination parameters were derived from our in-house experimental data. The equations were described (eqs S3, S20−S23). Other toxicokinetic parameters derived from our in-house experimental data were described in eqs S24−S25. Due to the absence of experimental values, the renal reabsorption parameters (e.g., Vmax_baso_invitro, Km_baso, Vmax_apical_invitro, and Km_apical) for both pregnant mice and fetus models were assumed to be the same as fitted values

https://doi.org/10.1021/acs.est.4c05405
Environ. Sci. Technol. 2024, 58, 18928−18939

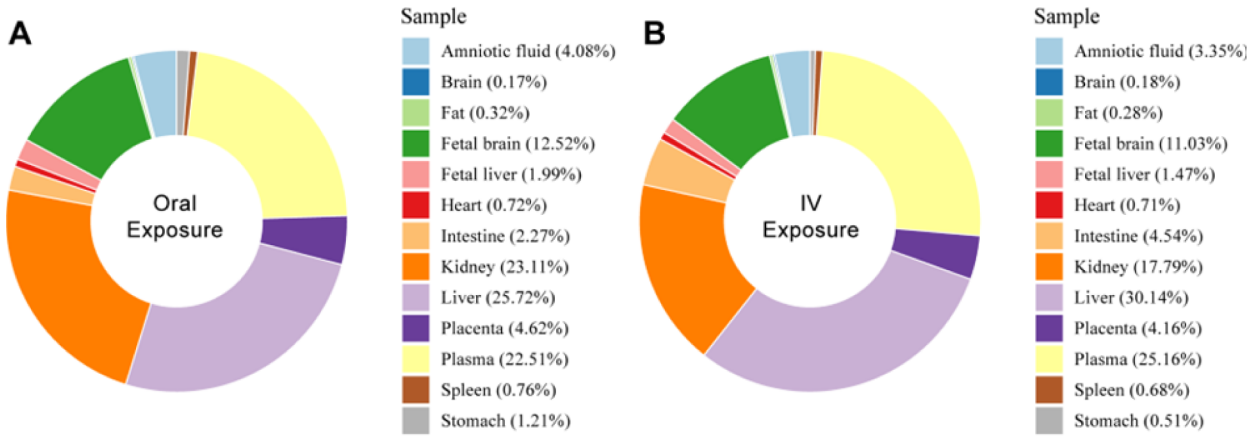

Figure 2. Percentage of F-53B accumulation in pregnant mice and fetal tissues after 96 h of exposure through (A) oral and (B) intravenous (IV) administrations. Different colors represent various tissues/organs and their respective accumulation percentages.

from previously published gestational PFOS PBPK models in rats and humans.[29] These reabsorption parameters were used to describe the Michaelis−Menten kinetic equation for understanding the renal handling of F-53B, including its reabsorption back into the bloodstream, which influences the overall clearance and retention. During model calibration, these parameters were set as initial values. Before model calibration, a sensitivity analysis was conducted to identify the most influential parameters. These identified parameters were subsequently optimized with observed TK profiles by using the Nelder−Mead approach implemented with the modFit function in the R package FME.[49] All collected and calibrated chemical-specific parameters for mouse and human models are presented in Table S7.

2.3.2. Model Evaluation and Sensitivity Analysis. The model calibration was conducted by comparing its predictions with observations from the independent evaluation data set, which consisted of an experimental TK data set excluded from calibration data (Table 1). Model performance was evaluated through statistical criteria and goodness-of-fit analysis in accordance with the PBPK model guidance published by the World Health Organization (WHO).[50] The goodness-of-fit analysis involved calculating the coefficient of determination (R^2) from a linear regression of log-transformed observed versus predicted values for both the calibration and evaluation data sets. The model was considered valid and acceptable if the predicted toxicokinetic profiles matched the observed values, and the predictions fell within a 2-fold range of the experimental data.

To identify the most sensitive parameters that significantly influence model simulations (e.g., selected dose metrics), we conducted local sensitivity analyses. This analysis aimed to determine which model parameters had high impacts on maternal and fetal areas under the curves (AUC) in plasma. Specifically, the AUCs were derived from the gestational model in mice following a single oral dose of 80 μg/kg/day and in humans following a daily dose of 0.122 ng/kg/day over a pre-pregnancy duration of 30 years and a pregnancy duration of 40 weeks. Each parameter was varied by 1% of its original value to assess its effect on the model output, and the normalized sensitivity coefficient (NSC) was calculated.[31,35,36,51] An absolute NSC value of ≥30% was considered indicative of significant influence.[29] The detailed equations are provided eqs S26−S27.

2.4. Human PBPK Model Extrapolation and Monte Carlo Analysis. The structure of the PBPK model for F-53B in pregnant women was consistent with that of the mice model. Once the mouse PBPK model was calibrated, we extrapolated its application to humans by adjusting it to reflect differences between species in physiological and chemical-specific parameters. This involved replacing the physiological parameters, such as tissue volume and blood flow in mice, with corresponding parameters for humans (Table S4). While mice had an average body weight of 0.025 kg in experimental measurements, humans were assumed to be 60 kg. Several rate constants (k) in humans including absorption, elimination, and renal reabsorption parameters (Table S7) were estimated using an allometric scaling equation.[52]

$$k_{human} = k_{mouse} \cdot \left(\frac{BW_{human}}{BW_{mouse}}\right)^{-0.25}$$

where k_{human} and k_{mouse} are the rate constants in humans and mouse, respectively. BW_{human} and BW_{mouse} refer to the body weight in humans and mice, respectively, and −0.25 is the allometric exponent. In addition, the human biomonitoring data sets obtained from the literature (refer to Table S10) were used to validate the human PBPK model. Given the limited availability of detailed human population exposure information, exposure doses were determined based on Estimated daily intakes (EDIs) reported in the literature, ranging from 0.067 ng/kg/day to 1.87 ng/kg/day (Table S8). Utilizing these exposure doses, predicted values were obtained by simulating exposure from birth to 30 years along with 38 weeks of pregnancy (collection time points for most biomonitoring data sets) and subsequently compared with measured data. The detailed assumption was provided in Section S7.

Monte Carlo analyses were applied to pregnancy PBPK models of humans to characterize the uncertainty and interindividual variability of parameters on model output. Only influential parameters (i.e., parameters with NSC values ≥30%) and calibration parameter values were included in the Monte Carlo analyses, with their mean values considered as the central tendency of the distributions (Table S9). The parameter values were then randomly sampled based on predefined probability distributions from previous studies.[28,29,34] Each parameter distribution was truncated at the 2.5th and 97.5th percentiles to establish the upper and lower bounds (Table S9), with the details described (Section S8).[34]

https://doi.org/10.1021/acs.est.4c05405
Environ. Sci. Technol. 2024, 58, 18928−18939

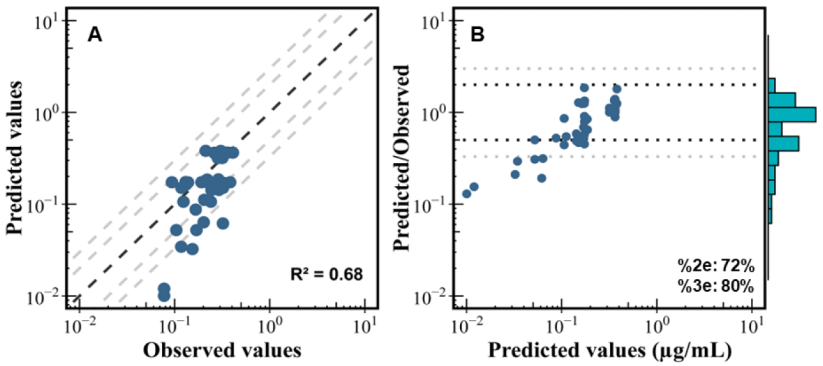

Figure 3. Overall model calibration and evaluation results. (A) Global evaluation of the goodness of model fit between the observed (*x*-axis) and predicted values (*y*-axis) and (B) predicted-to-observed ratios versus predicted values plot for F-53B in pregnant mice. In plot B, the histogram represents the distribution of predicted-to-observed ratios. The abbreviation R^2 represents the adjusted determination coefficients estimated based on calibration data sets. The %2e and %3e indicate the percentage of predicted values was within a 2 and 3-fold error range, respectively.

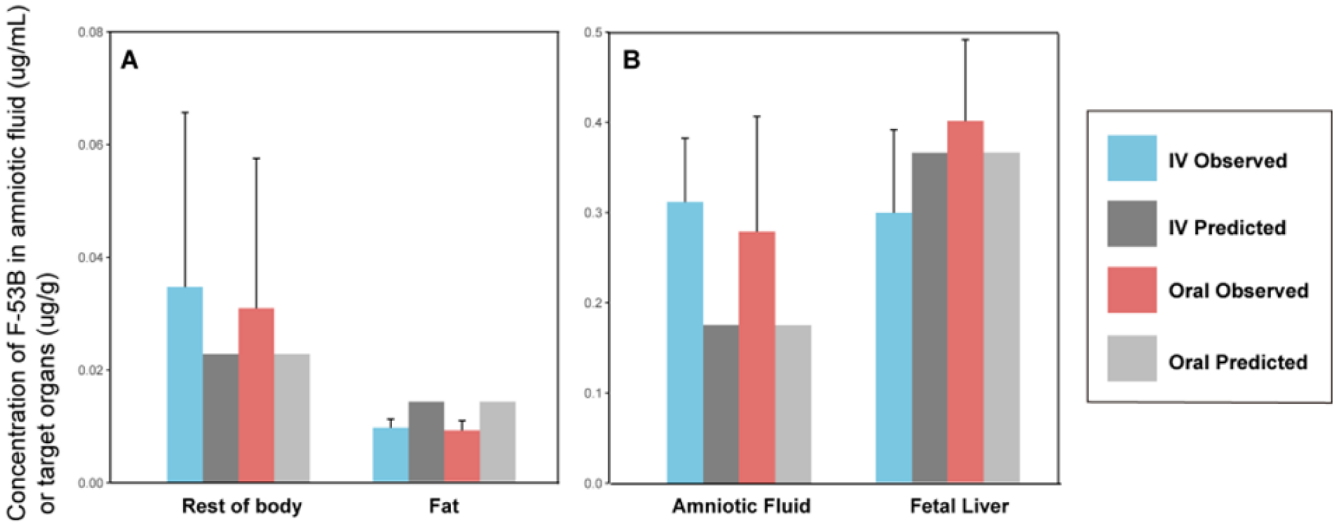

Figure 4. Comparison of model predictions with in-house experimental data (mean ± SD). (A) Mother (fat and rest of body) and (B) fetus (amniotic fluid and fetal liver) at 96 h postexposure.

2.5. Code Availability and Result Reproducibility. The PBPK model was implemented by using the R package "mrgsolve".[53] Ordinary differential equations (ODEs) were written in FORTRAN and solved by the DLSODA solver to significantly speed up the calculations. The model code, along with all data sets utilized for calibration and evaluation of the present PBPK models, can be downloaded from GitHub at the following link: https://github.com/choulab210.

3. RESULTS

3.1. Pharmacokinetic Data. The temporal trends of F-53B in pregnant and fetal mice administered orally and intravenously are shown in Figure S2, with the peak plasma concentrations occurring at 24 h (0.25 μg/mL) and 8 h (0.37 μg/mL) in pregnant mice. Figure 2 shows the accumulation of F-53B in organs and body fluids after 96 h of administration. The accumulations of F-53B in selected tissue/organs through the oral (O) and IV administration routes were as follows: liver (O: 25.72%, IV: 30.14%) > plasma (O: 22.51%, IV: 25.16%) ≈ kidney (O: 17.79%, IV: 23.11%) > fetal brain (O: 11.03%, IV: 12.52%) > placenta (O: 4.16%, IV: 4.62%) ≈ amniotic fluid (O: 3.35%, IV: 4.08%) ≈ intestine (O: 2.27%, IV: 4.54%) > fetal liver (O: 1.47%, IV: 1.99%) > other tissues (O: 0.17%, IV: 1.21%), which indicated that the liver was the target organ of F-53B accumulation in pregnant mice, and the fetal brain was the main organ in the fetus. Using protein binding assays, we found that F-53B was highly bound to plasma proteins, with a binding ratio of 98.70% ± 0.56% and 99.54% ± 0.19% by oral and intravenous administration, respectively (Table S11). In addition, after administration of 80 μg/kg F-53B to pregnant mice for 96 h, the excreted percentage via urine was 33.72% ± 4.65% and 32.55% ± 4.25%, respectively, and via feces was 2.30% ± 1.39% and 2.81% ± 0.38%, respectively. The clearance was determined to be 2.33 ± 1.21 and 1.82 ± 1.08 mL/h/kg. Other TK parameters were summarized in Table S12.

3.2. Model Calibration and Evaluation for Mice. The F-53B PBPK model, developed based on oral and IV administration corresponding to in-house pharmacokinetic studies, was calibrated with F-53B concentrations in plasma and target organ concentrations (e.g., maternal plasma, maternal liver, and fetal brain) of pregnant and fetal mice. Global goodness-of-fit was evaluated by comparing model predictions against observed values and estimating the residual between predictions and observations (Figure 3). The model demonstrated satisfactory performance on both calibration and evaluation data set measured in pregnant and fetal mice, with an adjusted coefficient of determination (R^2) of 0.68.

https://doi.org/10.1021/acs.est.4c05405
Environ. Sci. Technol. 2024, 58, 18928−18939

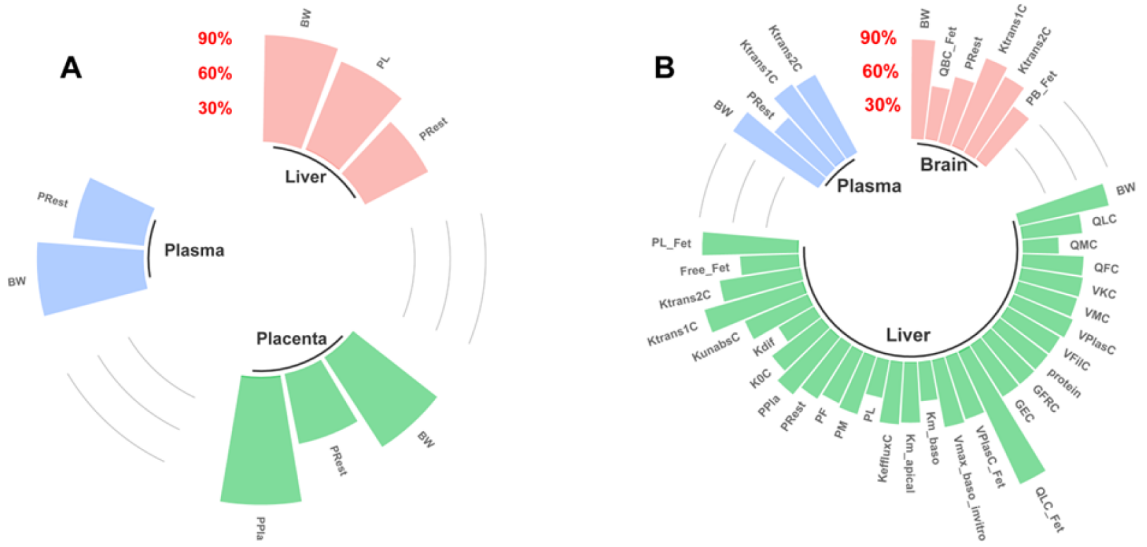

Figure 5. Normalized sensitivity coefficients (NSCs) of optimized parameters using the area under curves (AUCs) of F-53B in (A) plasma, liver, and placenta in the pregnant mice, and (B) plasma, brain, and liver in the fetal mice after a single oral dose of 80 μg/kg/day on GD13. Only parameters with NSC $\geq$ 0.3 are shown in the plots.

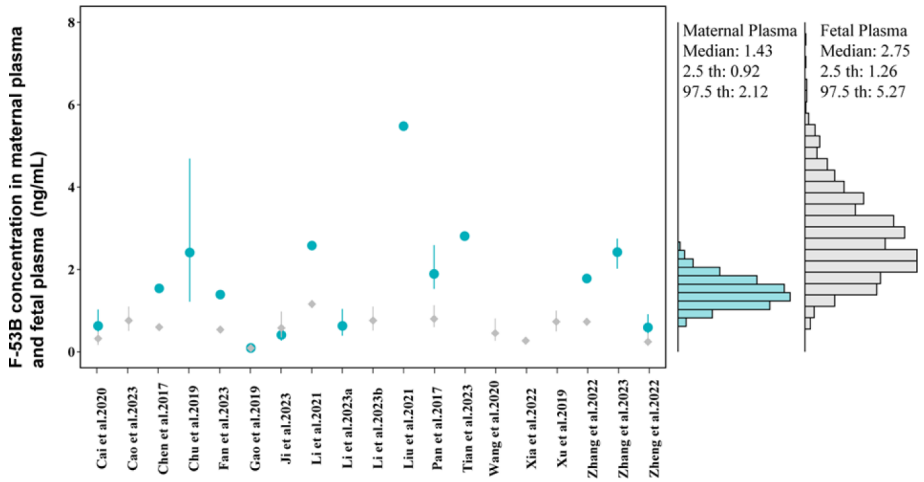

Figure 6. Histogram of simulated concentrations compared with measured values of F-53B concentration. The figure compares simulated concentrations with measured values (mean ± SD) in maternal plasma (blue circles) and cord blood (gray diamonds) reported in different studies and various human populations in China. The corresponding numeric data are available in Table S9.

Additionally, the percentages of the predicted values within 2- and 3-fold errors were 72% and 80%, respectively. These results indicated that over 72% and 80% of model predictions fell within 2- and 3-fold error ranges of measured data, respectively. However, the model underpredicts the lower concentrations at later time points, suggesting that an elimination mechanism may not be properly accounted for or calibrated.

The simulated results predicted by the calibrated PBPK model were compared with measured values in the plasma, liver, and fetal brain from calibration pharmacokinetic data through oral and IV administration (Figure S3A–F). The time-course concentration profiles for F-53B exhibit visual consistency with the measured values in plasma through oral administration (Figure S3A), as well as in the liver and fetal brain through both oral (Figures S3B,C) and IV administrations (Figure S3E,F). However, the model appears to underestimate the concentration of plasma following IV administration (Figure S3D). In addition, as shown in Figure 4 for evaluation data, model simulations at 96 h postexposure for fat and rest of body in pregnant mice and amniotic fluid and liver in fetal mice through oral or IV administration agreed with most of the data set. (The model simulations at different time points were presented in Figure S4). Overall, these findings indicate that the model adequately simulates both calibration and evaluation data sets.

3.3. Sensitivity Analysis. The local sensitivity analysis was conducted based on the dose metrics of 96-h AUCs of F-53B concentration in plasma, liver, and placenta in pregnant mice and in plasma, brain, and liver in fetal mice. Figure 5 is a representative figure displaying the parameters with absolute values of NSCs $\geq$ 0.3 in the mouse gestational models. The complete sensitivity analysis results for all parameters can be found in Table S13. The results showed that the body weight (BW) and partition coefficients in the rest of body (PRest) had a significant influence across maternal plasma, liver, and placenta AUC in mice. Similarly, the partition coefficient of liver and placenta significantly impacts the predictions of liver

https://doi.org/10.1021/acs.est.4c05405
Environ. Sci. Technol. 2024, 58, 18928−18939

and placental AUC. In fetuses, beyond these maternal parameters, the placental transfer rate constants (Ktrans1C and Ktrans2C) notably impact the AUCs of plasma, brain, and liver tissues in the fetal mouse. Notably, the liver blood flow (QLC_Fet) and brain blood flow (QBC_Fet) were significant determinants of the liver AUC and brain AUC in fetal mice.

3.4. Extrapolation of PBPK Model from Mice to Humans. The PBPK model developed for pregnant mice was extrapolated to humans, and population simulations (1000 individuals) were generated by varying relevant physiological parameters with Monte Carlo simulations. By considering possible exposure scenarios and doses (the EDIs of F-53B range from 0.067 to 1.87 ng/kg/day, simulated at 0.122 ng/kg/day for a 30-year exposure along with 38 weeks of pregnancy) (Table S8), which was obtained from literature,[54−58] the human gestational PBPK model was simulated to compare with the human biomonitoring data during pregnancy (Figure 6). The results indicated that the median values (1.43 ng/mL) of simulated F-53B concentrations in human populations with a range of predictions (range: 0.92−2.12) were quite close to the values of biomonitoring data obtained from the literature[8,9,11,18,19,21,22,25,59−69] in maternal plasma (median: 1.66 ng/mL and range: 0.094−5.48 ng/mL). However, the predicted cord blood concentration (median: 0.59 and range: 0.091−1.16 ng/mL) underestimated the measured concentration (median: 2.75 and range: 1.26−5.27 ng/mL).

4. DISCUSSION

This study comprehensively investigated the toxicokinetics of F-53B, a substitute for PFOS, in pregnant mice to address the gaps in the sparse existing data. Building on previous modeling efforts, a PBPK model for pregnant mice was developed, and subsequently, the model was extrapolated to pregnant women to enhance the utility of our findings for risk assessment in susceptible populations. The integration of Monte Carlo simulations has enabled the model to account for variability and uncertainty in the sensitive and estimated parameters. The accuracy of our predictions, validated by human biomonitoring data, underscores our model's ability to assess risks to sensitive populations, such as pregnant women and the fetus. Additionally, our work lays the groundwork for extending these modeling approaches to other PFAS chemicals, expanding the scope of risk assessment for emerging contaminants.

4.1. Sensitivity Analysis. This study indicated that the model parameters' sensitivities differed between the maternal and fetal PBPK models. In the maternal model, the most sensitive parameters to F-53B levels were the body weight and partition coefficients of the respective predicted tissues. These findings highlighted the impacts of changes in physiological and physicochemical parameters during pregnancy on the distribution of F-53B. Specifically, increased body weight during pregnancy can change the volume of distribution and metabolic and clearance rates, which are essential considerations for dosimetry adjustment in derivative guidance levels (i.e., reference dose) for pregnant populations. Moreover, the partition coefficients were notably impactful, indicating unique distribution characteristics that might modify F-53B exposure during pregnancy, which highlight the necessity of specific modeling of F-53B distribution in target tissues to better predict the chemical levels and potential toxicities. For the fetal model, the most sensitive parameters were the bidirectional placental transfer rate constants (Ktrans1C and Ktrans2C), which determine the rate and extent of F-53B transfer between the mother and fetus. These findings are consistent with previous studies in PFOS in rats and humans,[29,31,35] and highlight similar mechanisms of transplacental effects of PFOS and F-53B. However, unlike in previous PFOS studies where renal reabsorption and excretion parameters were frequently sensitive,[29] these parameters do not play a key role in our F-53B models. This distinction might reflect the differences in the pharmacokinetic properties between PFOS and F-53B, suggesting F-53B may interact differently with renal transport proteins not similar to PFOS. While the sensitivity analysis may suggest that the renal parameters are not as critical for F-53B, the model's underprediction of elimination-phase concentrations (Figure 2) adds uncertainty to these results. This highlights the need for further investigation into renal elimination mechanisms and suggests that additional data on renal clearance and metabolism of F-53B could improve the model accuracy. Our findings are critical for developing specific models for F-53B in the pregnant population that reflect the specific pharmacokinetic properties of F-53B during pregnancy.

4.2. Model Evaluation and Extrapolation. Although the current mice model can adequately simulate most available data, it has slight uncertainties when extrapolating to humans. The human model was extrapolated from the mice model and compared to multiple biomonitoring studies. Due to the biomonitoring data being collected from different regions in China and lacking detailed historical exposure information, estimating the exposure doses and sources of F-53B is uncertain. To account for population variability based on various exposure scenarios (the EDIs of F-53B ranged from 0.067 to 1.87 ng/kg/day, and were simulated at 0.122 ng/kg/day for 30 years prepregnancy along with 38 weeks of pregnancy),[54−58] the population exposure to F-53B was simulated by integrating the PBPK model with the MC simulation. The simulated values were then compared with the observed maternal plasma and cord blood levels from human biomonitoring studies.[8,9,11,18,19,21,22,25,59−69] As shown in Figure 5, the estimated F-53B levels (median value: 1.44 ng/mL) in maternal plasma are well in agreement with the observed values (median value: 1.66 ng/mL) but the model slightly overestimated levels in cord blood (predicted median value: 2.76 ng/mL vs observed median value: 0.59 ng/mL). The reason for the overestimation is currently unknown, but it may be attributed to factors, such as potential differences in placental transfer rates, fetal metabolism, or inaccuracies in the estimated exposure scenarios. Additionally, the parameters used in the human model were extrapolated from the mice model using surface area scaling, which may not fully account for interspecies differences between humans and mice. Further refinement of the model parameters, especially those related to placental transport and fetal distribution, will help adjust our prediction more closely to observed data. Continued investigation is required to understand and address these uncertainties.

4.3. Potential Application in Risk Assessment. The physiological and biochemical parameters make significant changes during pregnancy, influencing the ADME properties of chemicals and highlighting the necessity for adjustment when deriving reference doses for sensitive populations. This study developed the first PBPK model for F-53B in pregnant mice and humans, incorporating physiological processes, such as transporter-mediated renal reabsorption/excretion and dynam-

https://doi.org/10.1021/acs.est.4c05405
Environ. Sci. Technol. 2024, 58, 18928−18939

ic changes in physiological parameters during pregnancy. Our model provides a framework for understanding the relationship between maternal exposure and infant target tissue dose, enhancing the science of assessing F-53B exposure and associated health risks among sensitive populations. Extrapolating the model from pregnant mice to humans helps to depict the relationship between external and internal levels in pregnant women and fetuses at different developmental stages. Although several studies have investigated the reproductive, developmental, and neural toxicity of F-53B,[70] many are not representative, and the evidence remains insufficient. After clarifying the association and mechanism, based on epidemiological studies and toxic effect studies in mice, the present PBPK model can be used to calculate the reference dose of F-53B exposure in pregnant women and assess the associated health risk.

4.4. Limitations. Several limitations need to be addressed in interpreting our results. First, due to the lack of toxicokinetic/toxicodynamic information in pregnant mice and fetuses, our model was not well-fitted and could not be further parametrized. Some chemical-specific parameters were retained from our previous PFOS models[28,29] instead of using F-53B-specific. Although F-53B has a similar structure and function to PFOS, there are differences in binding to various proteins, such as HSA, OAT, and urate transporter 1 (URAT1).[71] Second, the elimination mechanisms, including enterohepatic circulation and metabolism of F-53B, were not described in the current model, which led to the underprediction of the lower concentration in our model (Figures 2 and S3). Our model assumed that F-53B excreted via bile will move to the feces directly rather than returning to the small intestine for potential enterohepatic circulation. However, recent studies have shown that long-chain PFAS, such as PFOS, can bind to the apical sodium-dependent bile acid transporter (ASBT, Slc10a2) and the Na^+−taurocholate cotransport polypeptide (NTCP, Slc10a1), which may be responsible for the maintenance of high concentrations in the liver.[72] Yi et al.[73] reported that 6:2 Cl-PFESA is susceptible to reductive dichlorination in rats (13.6% transformation in the liver) to form persistent 6:2 H-PFESA. However, these physicochemical mechanisms have all failed to be added to the model due to a lack of detailed parametric descriptions of the key transporter proteins. Third, due to a lack of TK data and parameters from experiments on pregnant women and their fetuses, placental transport was described as a bidirectional passive diffusion process without adding the active transport possibly mediated by OAT4.[60,64] In addition, some of the chemical-specific parameters of the fetus were assumed to be identical with those of the mother. Although we calibrated these parameters with internal exposure levels, the biological reliability of the model would be improved if placental transport and fetal chemical parameters for F-53B were obtained by using experiments in vivo and in vitro. Examples of such studies include those by Personne et al.,[74] who investigated placental transport parameters for *cis*- and *trans*-permethrin as well as fetal partition coefficients using in vivo assays, and by Ke et al.,[75] who incorporated in vitro-calculated cytochrome P450 3A4 enzyme concentrations in a pregnancy PBPK model to better fit the elimination of antenatal corticosteroids. These studies demonstrate the feasibility of using in vivo and in vitro approaches to obtain relevant data for improving the model accuracy. Fourth, for the gestational PBPK modeling in humans, since exposure information is not fully available over time and across regions, we assumed that humans were exposed constantly and simulated internal exposure concentrations in pregnant women using EDIs reported (Table S8). This simulation method had been successfully applied to PBPK modeling of PFOS,[29] and the plasma biomonitoring concentrations of pregnant women were within the range of our simulations. Fifth, we acknowledge that the assumptions on the Monte Carlo simulation about parameter distributions, such as physiological parameters being normally distributed and partition coefficients, rate constants, and other chemical-specific parameters being log-normally distributed, are based on commonly used practices but lack strong empirical support. The default coefficients of variation were set to 20% for partition coefficients and 30% for physiological and other chemical-specific parameters. These assumptions could potentially impact the results and conclusions of our study. A recent study[76] has shown, that different assumptions about parameter distributions can significantly influence the outcomes of Monte Carlo PBPK modeling, especially for sensitive subpopulations. Future studies should explore the sensitivity of model predictions to these assumptions and consider incorporating empirical data to better define parameter distributions. Finally, the potential oversimplification of time-varying physiological changes may present a flaw and limitation in sensitivity analysis (Section S7) and Monte Carlo simulation (Section S8). In sensitivity analysis, using the baseline parameter value instead of time-varying parameters to estimate the impact of changes on model outputs may overlook critical variations at different time points. Future studies should aim to refine this approach by incorporating more detailed data on the trajectories of time-varying parameters and their impacts at different stages of the simulation. Additionally, by only considering the variability in baseline physiological parameter values and updating physiological values using the same growth equations, we may not account for all individual variability and complex interactions in physiological processes. The growth equations might differ across various populations and individual cases, representing general trends but failing to capture the variability in growth among different populations. Further investigation and refinement of the model are feasible if more detailed data becomes available.

■ ASSOCIATED CONTENT

Supporting Information

The Supporting Information is available free of charge at https://pubs.acs.org/doi/10.1021/acs.est.4c05405.

Toxicokinetic study in pregnant mice; protein binding assay; equations and code for the pregnancy PBPK model; calculation of chemical-specific parameters; toxicokinetic parameters; sensitivity analysis; Monte Carlo simulations; target analytes' information; instruments and reagents; model parameters description of gestational PBPK model of mice and humans; population estimated daily intakes (EDIs) for F-53B; values and parameter distributions used in the Monte Carlo analysis for the gestational; maternal plasma and cord blood biomonitoring data; F-53B plasma protein binding ratio (mean ± SEM); pharmacokinetic parameters of F-53B following oral or IV administration in pregnant mice; sensitive parameters identified by the local sensitivity analysis; plot of simulated values of

https://doi.org/10.1021/acs.est.4c05405
Environ. Sci. Technol. 2024, 58, 18928−18939

growth equations versus experimental values of body weight; experimental concentrations of F-53B via oral and IV administrations in maternal and fetal mice; fitting plot between model predictions and observed values; comparison of model predictions of fetal liver with in-house experimental data (PDF)

AUTHOR INFORMATION

Corresponding Authors

Xiaowen Zeng − *Joint International Research Laboratory of Environment and Health, Ministry of Education, Guangdong Provincial Engineering Technology Research Center of Environmental Pollution and Health Risk Assessment, Department of Occupational and Environmental Health, School of Public Health, Sun Yat-sen University, Guangzhou 510080, China;* orcid.org/0000-0003-3918-1841; Email: zxw63@mail.sysu.edu.cn

Wei-Chun Chou − *Department of Environmental Sciences, University of California, Riverside, California 92521, United States; Environmental Toxicology Graduate Program, University of California, Riverside, California 92521, United States;* orcid.org/0000-0003-3355-6921; Email: weichunc.chou@ucr.edu

Authors

Jing Zhang − *Joint International Research Laboratory of Environment and Health, Ministry of Education, Guangdong Provincial Engineering Technology Research Center of Environmental Pollution and Health Risk Assessment, Department of Occupational and Environmental Health, School of Public Health, Sun Yat-sen University, Guangzhou 510080, China*

Shen-Pan Li − *Joint International Research Laboratory of Environment and Health, Ministry of Education, Guangdong Provincial Engineering Technology Research Center of Environmental Pollution and Health Risk Assessment, Department of Occupational and Environmental Health, School of Public Health, Sun Yat-sen University, Guangzhou 510080, China*

Qing-Qing Li − *Acacia Lab for Implementation Science, Institute for Global Health, Dermatology Hospital of Southern Medical University, Guangzhou 510515, China*

Yun-Ting Zhang − *Joint International Research Laboratory of Environment and Health, Ministry of Education, Guangdong Provincial Engineering Technology Research Center of Environmental Pollution and Health Risk Assessment, Department of Occupational and Environmental Health, School of Public Health, Sun Yat-sen University, Guangzhou 510080, China*

Guang-Hui Dong − *Joint International Research Laboratory of Environment and Health, Ministry of Education, Guangdong Provincial Engineering Technology Research Center of Environmental Pollution and Health Risk Assessment, Department of Occupational and Environmental Health, School of Public Health, Sun Yat-sen University, Guangzhou 510080, China;* orcid.org/0000-0002-2578-3369

Alexa Canchola − *Department of Environmental Sciences, University of California, Riverside, California 92521, United States; Environmental Toxicology Graduate Program, University of California, Riverside, California 92521, United States;* orcid.org/0000-0001-8285-4795

Complete contact information is available at: https://pubs.acs.org/10.1021/acs.est.4c05405

Notes

The authors declare no competing financial interest.

ACKNOWLEDGMENTS

This study was supported by the National Science Foundation of China (No. 82073503), the Natural Science Foundation of Guangdong Province (No. 2021B1515020015), the Guangzhou Science and Technology Project (No. 2024A04J6476), and the University of California, Riverside College of Natural & Agricultural Sciences New Faculty Startup funds.

REFERENCES

(1) Wang, S.; Huang, J.; Yang, Y.; Hui, Y.; Ge, Y.; Larssen, T.; Yu, G.; Deng, S.; Wang, B.; Harman, C. First Report of a Chinese PFOS Alternative Overlooked for 30 Years: Its Toxicity, Persistence, and Presence in the Environment. *Environ. Sci. Technol.* **2013**, *47* (18), 10163−10170.

(2) Liu, L.-S.; Guo, Y.-T.; Wu, Q.-Z.; Zeeshan, M.; Qin, S.-J.; Zeng, H.-X.; Lin, L.-Z.; Chou, W.-C.; Yu, Y.-J.; Dong, G.-H.; et al. Per- and Polyfluoroalkyl Substances in Ambient Fine Particulate Matter in the Pearl River Delta, China: Levels, Distribution and Health Implications. *Environ. Pollut.* **2023**, *334*, 122138.

(3) Liu, W.; Qin, H.; Li, J.; Zhang, Q.; Zhang, H.; Wang, Z.; He, X. Atmospheric Chlorinated Polyfluorinated Ether Sulfonate and Ionic Perfluoroalkyl Acids in 2006 to 2014 in Dalian, China. *Environ. Toxicol. Chem.* **2017**, *36* (10), 2581−2586.

(4) Pan, Y.; Zhang, H.; Cui, Q.; Sheng, N.; Yeung, L. W. Y.; Sun, Y.; Guo, Y.; Dai, J. Worldwide Distribution of Novel Perfluoroether Carboxylic and Sulfonic Acids in Surface Water. *Environ. Sci. Technol.* **2018**, *52* (14), 7621−7629.

(5) Wei, C.; Wang, Q.; Song, X.; Chen, X.; Fan, R.; Ding, D.; Liu, Y. Distribution, Source Identification and Health Risk Assessment of PFASs and Two PFOS Alternatives in Groundwater from Non-Industrial Areas. *Ecotoxicol. Environ. Saf.* **2018**, *152*, 141−150.

(6) MacInnis, J. J.; Lehnherr, I.; Muir, D. C. G.; Quinlan, R.; De Silva, A. O. Characterization of Perfluoroalkyl Substances in Sediment Cores from High and Low Arctic Lakes in Canada. *Sci. Total Environ.* **2019**, *666*, 414−422.

(7) Wang, Y.; Shi, Y.; Vestergren, R.; Zhou, Z.; Liang, Y.; Cai, Y. Using Hair, Nail and Urine Samples for Human Exposure Assessment of Legacy and Emerging per- and Polyfluoroalkyl Substances. *Sci. Total Environ.* **2018**, *636*, 383−391.

(8) Chen, F.; Yin, S.; Kelly, B. C.; Liu, W. Chlorinated Polyfluoroalkyl Ether Sulfonic Acids in Matched Maternal, Cord, and Placenta Samples: A Study of Transplacental Transfer. *Environ. Sci. Technol.* **2017**, *51* (11), 6387−6394.

(9) Chu, C.; Zhou, Y.; Li, Q. Q.; Bloom, M. S.; Lin, S.; Yu, Y. J.; Chen, D.; Yu, H. Y.; Hu, L. W.; Yang, B. Y.; Zeng, X. W.; Dong, G. H. Are Perfluorooctane Sulfonate Alternatives Safer? New Insights from a Birth Cohort Study. *Environ. Int.* **2020**, *135*, 105365.

(10) Awad, R.; Zhou, Y.; Nyberg, E.; Namazkar, S.; Yongning, W.; Xiao, Q.; Sun, Y.; Zhu, Z.; Bergman, Å.; Benskin, J. P. Emerging Per- and Polyfluoroalkyl Substances (PFAS) in Human Milk from Sweden and China. *Environ. Sci. Process Impacts* **2020**, *22* (10), 2023−2030.

(11) Ji, D.; Pan, Y.; Qiu, X.; Gong, J.; Li, X.; Niu, C.; Yao, J.; Luo, S.; Zhang, Z.; Wang, Q.; Dai, J.; Wei, Y. Unveiling Distribution of Per- and Polyfluoroalkyl Substances in Matched Placenta-Serum Tetrads: Novel Implications for Birth Outcome Mediated by Placental Vascular Disruption. *Environ. Sci. Technol.* **2023**, *57* (14), 5782−5793.

(12) Li, S.; Wu, L. Y.; Zeng, H. X.; Zhang, J.; Qin, S. J.; Liang, L. X.; Andersson, J.; Meng, W. J.; Chen, X. Y.; Wu, Q. Z.; Lin, L. Z.; Chou, W. C.; Dong, G. H.; Zeng, X. W. Hepatic Injury and Ileitis Associated with Gut Microbiota Dysbiosis in Mice upon F−53B Exposure. *Environ. Res.* **2024**, *248*, 118305.

(13) Liang, L. X.; Liang, J.; Li, Q. Q.; Zeeshan, M.; Zhang, Z.; Jin, N.; Lin, L. Z.; Wu, L. Y.; Sun, M. K.; Tan, W. H.; Zhou, Y.; Chu, C.; Hu, L. W.; Liu, R. Q.; Zeng, X. W.; Yu, Y.; Dong, G. H. Early Life Exposure to F-53B Induces Neurobehavioral Changes in Developing Children and Disturbs Dopamine-Dependent Synaptic Signaling in Weaning Mice. *Environ. Int.* **2023**, *181*, 108272.
(14) Wu, L.; Zeeshan, M.; Dang, Y.; Zhang, Y. T.; Liang, L. X.; Huang, J. W.; Zhou, J. X.; Guo, L. H.; Fan, Y. Y.; Sun, M. K.; Yu, T.; Wen, Y.; Lin, L. Z.; Liu, R. Q.; Dong, G. H.; Chu, C. Maternal Transfer of F-53B Inhibited Neurobehavior in Zebrafish Offspring Larvae and Potential Mechanisms: Dopaminergic Dysfunction, Eye Development Defects and Disrupted Calcium Homeostasis. *Sci. Total Environ.* **2023**, *894*, 164838.
(15) Goudarzi, H.; Nakajima, S.; Ikeno, T.; Sasaki, S.; Kobayashi, S.; Miyashita, C.; Ito, S.; Araki, A.; Nakazawa, H.; Kishi, R. Prenatal Exposure to Perfluorinated Chemicals and Neurodevelopment in Early Infancy: The Hokkaido Study. *Sci. Total Environ.* **2016**, *541*, 1002−1010.
(16) Lien, G. W.; Huang, C. C.; Shiu, J. S.; Chen, M. H.; Hsieh, W. S.; Guo, Y. L.; Chen, P. C. Perfluoroalkyl Substances in Cord Blood and Attention Deficit/Hyperactivity Disorder Symptoms in Seven-Year-Old Children. *Chemosphere* **2016**, *156*, 118−127.
(17) Waterland, R. A.; Michels, K. B. Epigenetic Epidemiology of the Developmental Origins Hypothesis. *Annu. Rev. Nutr.* **2007**, *27*, 363−388.
(18) Zheng, P.; Liu, Y.; An, Q.; Yang, X.; Yin, S.; Ma, L. Q.; Liu, W. Prenatal and Postnatal Exposure to Emerging and Legacy Per-/Polyfluoroalkyl Substances: Levels and Transfer in Maternal Serum, Cord Serum, and Breast Milk. *Sci. Total Environ.* **2022**, *812*, 152446.
(19) Tian, Y.; Zhou, Q.; Zhang, L.; Li, W.; Yin, S.; Li, F.; Xu, C. In Utero Exposure to Per-/Polyfluoroalkyl Substances (PFASs): Preeclampsia in Pregnancy and Low Birth Weight for Neonates. *Chemosphere* **2023**, *313*, 137490.
(20) Xu, C.; Zhang, L.; Zhou, Q.; Ding, J.; Yin, S.; Shang, X.; Tian, Y. Exposure to Per- and Polyfluoroalkyl Substances as a Risk Factor for Gestational Diabetes Mellitus through Interference with Glucose Homeostasis. *Sci. Total Environ.* **2022**, *838*, 156561.
(21) Zhang, Y.; Chen, R.; Gao, Y.; Qu, J.; Wang, Z.; Zhao, M.; Bai, X.; Jin, H. Human Serum Poly- and Perfluoroalkyl Substance Concentrations and Their Associations with Gestational Diabetes Mellitus. *Environ. Pollut.* **2023**, *317*, 120833.
(22) Xu, C.; Yin, S.; Liu, Y.; Chen, F.; Zhong, Z.; Li, F.; Liu, K.; Liu, W. Prenatal Exposure to Chlorinated Polyfluoroalkyl Ether Sulfonic Acids and Perfluoroalkyl Acids: Potential Role of Maternal Determinants and Associations with Birth Outcomes. *J. Hazard. Mater.* **2019**, *380*, 120867.
(23) Liu, X.; Zhang, L.; Liu, J.; Zaya, G.; Wang, Y.; Xiang, Q.; Li, J.; Wu, Y. 6: 2 Chlorinated Polyfluoroalkyl Ether Sulfonates Exert Stronger Thyroid Homeostasis Disruptive Effects in Newborns than Perfluorooctanesulfonate: Evidence Based on Bayesian Benchmark Dose Values from a Population Study. *Environ. Sci. Technol.* **2023**, *57* (31), 11489−11498.
(24) Liu, H.; Pan, Y.; Jin, S.; Li, Y.; Zhao, L.; Sun, X.; Cui, Q.; Zhang, B.; Zheng, T.; Xia, W.; Zhou, A.; Campana, A. M.; Dai, J.; Xu, S. Associations of Per-/Polyfluoroalkyl Substances with Glucocorticoids and Progestogens in Newborns. *Environ. Int.* **2020**, *140*, 105636.
(25) Cao, Z.; Li, J.; Yang, M.; Gong, H.; Xiang, F.; Zheng, H.; Cai, X.; Xu, S.; Zhou, A.; Xiao, H. Prenatal Exposure to Perfluorooctane Sulfonate Alternatives and Associations with Neonatal Thyroid Stimulating Hormone Concentration: A Birth Cohort Study. *Chemosphere* **2023**, *311* (Pt 1), 136940.
(26) Zhou, Y.; Li, Q.; Wang, P.; Li, J.; Zhao, W.; Zhang, L.; Wang, H.; Cheng, Y.; Shi, H.; Li, J.; Zhang, Y. Associations of Prenatal PFAS Exposure and Early Childhood Neurodevelopment: Evidence from the Shanghai Maternal-Child Pairs Cohort. *Environ. Int.* **2023**, *173*, 107850.
(27) National Academies of Sciences, Engineering, and Medicine. *Building Confidence In New Evidence Streams For Human Health Risk Assessment*; National Academies of Sciences, Engineering, and Medicine, 2023. .
(28) Chou, W. C.; Lin, Z. Bayesian Evaluation of a Physiologically Based Pharmacokinetic (PBPK) Model for Perfluorooctane Sulfonate (PFOS) to Characterize the Interspecies Uncertainty between Mice, Rats, Monkeys, and Humans: Development and Performance Verification. *Environ. Int.* **2019**, *129*, 408−422.
(29) Chou, W. C.; Lin, Z. Development of a Gestational and Lactational Physiologically Based Pharmacokinetic (PBPK) Model for Perfluorooctane Sulfonate (PFOS) in Rats and Humans and Its Implications in the Derivation of Health-Based Toxicity Values. *Environ. Health Perspect* **2021**, *129* (3), 37004.
(30) Yang, C. H.; Glover, K. P.; Han, X. Characterization of Cellular Uptake of Perfluorooctanoate via Organic Anion-Transporting Polypeptide 1A2, Organic Anion Transporter 4, and Urate Transporter 1 for Their Potential Roles in Mediating Human Renal Reabsorption of Perfluorocarboxylates. *Toxicol. Sci.* **2010**, *117* (2), 294−302.
(31) Loccisano, A. E.; Campbell, J. L., Jr.; Butenhoff, J. L.; Andersen, M. E.; Clewell, H. J., III Evaluation of Placental and Lactational Pharmacokinetics of PFOA and PFOS in the Pregnant, Lactating, Fetal and Neonatal Rat Using a Physiologically Based Pharmacokinetic Model. *Reprod. Toxicol.* **2012**, *33* (4), 468−490.
(32) Yoon, M.; Schroeter, J. D.; Nong, A.; Taylor, M. D.; Dorman, D. C.; Andersen, M. E.; Clewell, H. J., III Physiologically Based Pharmacokinetic Modeling of Fetal and Neonatal Manganese Exposure in Humans: Describing Manganese Homeostasis during Development. *Toxicol. Sci.* **2011**, *122* (2), 297−316.
(33) Worley, R. R.; Fisher, J. Application of Physiologically-Based Pharmacokinetic Modeling to Explore the Role of Kidney Transporters in Renal Reabsorption of Perfluorooctanoic Acid in the Rat. *Toxicol. Appl. Pharmacol.* **2015**, *289* (3), 428−441.
(34) Worley, R. R.; Yang, X.; Fisher, J. Physiologically Based Pharmacokinetic Modeling of Human Exposure to Perfluorooctanoic Acid Suggests Historical Non Drinking-Water Exposures Are Important for Predicting Current Serum Concentrations. *Toxicol. Appl. Pharmacol.* **2017**, *330*, 9−21.
(35) Loccisano, A. E.; Longnecker, M. P.; Campbell, J. L., Jr; Andersen, M. E.; Clewell, H. J., III Development of PBPK Models for PFOA and PFOS for Human Pregnancy and Lactation Life Stages. *J. Toxicol. Environ. Health Part A* **2013**, *76* (1), 25−57.
(36) Yoon, M.; Nong, A.; Clewell, H. J.; Taylor, M. D.; Dorman, D. C.; Andersen, M. E. Evaluating Placental Transfer and Tissue Concentrations of Manganese in the Pregnant Rat and Fetuses after Inhalation Exposures with a PBPK Model. *Toxicol. Sci.* **2009**, *112* (1), 44−58.
(37) Yang, X.; Doerge, D. R.; Fisher, J. W. Prediction and Evaluation of Route Dependent Dosimetry of BPA in Rats at Different Life Stages Using a Physiologically Based Pharmacokinetic Model. *Toxicol. Appl. Pharmacol.* **2013**, *270* (1), 45−59.
(38) Qi, Z.; Whitt, I.; Mehta, A.; Jin, J.; Zhao, M.; Harris, R. C.; Fogo, A. B.; Breyer, M. D. Serial Determination of Glomerular Filtration Rate in Conscious Mice Using FITC-Inulin Clearance. *Am. J. Physiol. Renal Physiol.* **2004**, *286* (3), F590−6.
(39) Hanwell, A.; Linzell, J. L. The Time Course of Cardiovascular Changes in Lactation in the Rat. *J. Physiol.* **1973**, *233* (1), 93−109.
(40) Addis, T.; Poo, L. J.; Lew, W. The Quantities of Protein Lost by the Various Organs and Tissues of the Body during a Fast. *J. Biol. Chem.* **1936**, *115* (1), 111−116.
(41) Carter, A. M.; Gu, W. Cerebral Blood Flow in the Fetal Guinea-Pig. *J. Dev Physiol.* **1988**, *10* (2), 123−129.
(42) Haddad, S.; Restieri, C.; Krishnan, K. Characterization of Age-Related Changes in Body Weight and Organ Weights from Birth to Adolescence in Humans. *J. Toxicol Environ. Health Part A* **2001**, *64* (6), 453−464.
(43) Kapraun, D. F.; Wambaugh, J. F.; Setzer, R. W.; Judson, R. S. Empirical Models for Anatomical and Physiological Changes in a Human Mother and Fetus during Pregnancy and Gestation. *PLoS One* **2019**, *14* (5), No. e0215906.

https://doi.org/10.1021/acs.est.4c05405
Environ. Sci. Technol. 2024, 58, 18928−18939

(44) Hejtmancik, M. R.; Ryan, M. J.; Toft, J. D.; Persing, R. L.; Kurtz, P. J.; Chhabra, R. S. Hematological Effects in F344 Rats and B6C3F1Mice during the 13-Week Gavage Toxicity Study of Methylene Blue Trihydrate. *Toxicol. Sci.* **2002**, *65* (1), 126−134.
(45) Hsu, V.; de L. T. Vieira, M.; Zhao, P.; Zhang, L.; Zheng, J. H.; Nordmark, A.; Berglund, E. G.; Giacomini, K. M.; Huang, S.-M. Towards Quantitation of the Effects of Renal Impairment and Probenecid Inhibition on Kidney Uptake and Efflux Transporters, Using Physiologically Based Pharmacokinetic Modelling and Simulations. *Clin. Pharmacokinet.* **2014**, *53* (3), 283−293.
(46) Davies, B.; Morris, T. Physiological Parameters in Laboratory Animals and Humans. *Pharm. Res.* **1993**, *10* (7), 1093−1095.
(47) Brown, R. P.; Delp, M. D.; Lindstedt, S. L.; Rhomberg, L. R.; Beliles, R. P. Physiological Parameter Values for Physiologically Based Pharmacokinetic Models. *Toxicol. Ind. Health* **1997**, *13* (4), 407−484.
(48) Yang, X.; Doerge, D. R.; Teeguarden, J. G.; Fisher, J. W. Development of a Physiologically Based Pharmacokinetic Model for Assessment of Human Exposure to Bisphenol A. *Toxicol. Appl. Pharmacol.* **2015**, *289* (3), 442−456.
(49) Soetaert, K.; Petzoldt, T. Inverse Modelling, Sensitivity and Monte Carlo Analysis in R Using Package FME. *J. Stat. Software* **2010**, *33* (3), 1−28.
(50) WHO (World Health Organization). *Characterization and application of physiologically based phamacokinetic models in risk assessment*. https://iris.who.int/handle/10665/44495. accessed 2024 April 09.
(51) Lin, Z.; Fisher, J. W.; Ross, M. K.; Filipov, N. M. A Physiologically Based Pharmacokinetic Model for Atrazine and Its Main Metabolites in the Adult Male C57BL/6 Mouse. *Toxicol. Appl. Pharmacol.* **2011**, *251* (1), 16−31.
(52) Kim, S. J.; Shin, H.; Lee, Y. B.; Cho, H. Y. Sex-Specific Risk Assessment of PFHxS Using a Physiologically Based Pharmacokinetic Model. *Arch. Toxicol.* **2018**, *92* (3), 1113−1131.
(53) Elmokadem, A.; Riggs, M. M.; Baron, K. T. Quantitative Systems Pharmacology and Physiologically-Based Pharmacokinetic Modeling With Mrgsolve: A Hands-On Tutorial. *CPT: pharmacometrics Syst. Pharmacol.* **2019**, *8* (12), 883−893.
(54) Wang, Y.; Li, X.; Zheng, Z.; Shi, Y.; Cai, Y. Chlorinated Polyfluoroalkyl Ether Sulfonic Acids in Fish, Dust, Drinking Water and Human Serum: From External Exposure to Internal Doses. *Environ. Int.* **2021**, *157*, 106820.
(55) Jin, Q.; Shi, Y.; Cai, Y. Occurrence and Risk of Chlorinated Polyfluoroalkyl Ether Sulfonic Acids (Cl-PFESAs) in Seafood from Markets in Beijing, China. *Sci. Total Environ.* **2020**, *726*, 138538.
(56) Chen, X.; Feng, X.; Sun, X.; Li, Y.; Yang, Y.; Shan, G.; Zhu, L. Quantifying Indirect Contribution from Precursors to Human Body Burden of Legacy PFASs Based on Paired Blood and One-Week Duplicate Diet. *Environ. Sci. Technol.* **2022**, *56* (9), 5632−5640.
(57) Sun, Q.; Bi, R.; Wang, T.; Su, C.; Chen, Z.; Diao, J.; Zheng, Z.; Liu, W. Are There Risks Induced by Novel and Legacy Poly- and Perfluoroalkyl Substances in Coastal Aquaculture Base in South China. *Sci. Total Environ.* **2021**, *779*, 146539.
(58) Wang, Y.; Gao, X.; Liu, J.; Lyu, B.; Li, J.; Zhao, Y.; Wu, Y. Exposure to Emerging and Legacy Polyfluoroalkyl Substances in the Sixth Total Diet Study - China, 2016−2019. *China CDC Wkly* **2022**, *4* (9), 168−171.
(59) Pan, Y.; Zhu, Y.; Zheng, T.; Cui, Q.; Buka, S. L.; Zhang, B.; Guo, Y.; Xia, W.; Yeung, L. W.; Li, Y.; Zhou, A.; Qiu, L.; Liu, H.; Jiang, M.; Wu, C.; Xu, S.; Dai, J. Novel Chlorinated Polyfluorinated Ether Sulfonates and Legacy Per-/Polyfluoroalkyl Substances: Placental Transfer and Relationship with Serum Albumin and Glomerular Filtration Rate. *Environ. Sci. Technol.* **2017**, *51* (1), 634−644.
(60) Gao, K.; Zhuang, T.; Liu, X.; Fu, J.; Zhang, J.; Fu, J.; Wang, L.; Zhang, A.; Liang, Y.; Song, M.; Jiang, G. Prenatal Exposure to Per- and Polyfluoroalkyl Substances (PFASs) and Association between the Placental Transfer Efficiencies and Dissociation Constant of Serum Proteins-PFAS Complexes. *Environ. Sci. Technol.* **2019**, *53* (11), 6529−6538.
(61) Cai, D.; Li, Q. Q.; Chu, C.; Wang, S. Z.; Tang, Y. T.; Appleton, A. A.; Qiu, R. L.; Yang, B. Y.; Hu, L. W.; Dong, G. H.; Zeng, X. W. High Trans-Placental Transfer of Perfluoroalkyl Substances Alternatives in the Matched Maternal-Cord Blood Serum: Evidence from a Birth Cohort Study. *Sci. Total Environ.* **2020**, *705*, 135885.
(62) Wang, J.; Pan, Y.; Wei, X.; Dai, J. Temporal Trends in Prenatal Exposure (1998−2018) to Emerging and Legacy Per- and Polyfluoroalkyl Substances (PFASs) in Cord Plasma from the Beijing Cord Blood Bank, China. *Environ. Sci. Technol.* **2020**, *54* (20), 12850−12859.
(63) Li, Y.; Lu, X.; Yu, N.; Li, A.; Zhuang, T.; Du, L.; Tang, S.; Shi, W.; Yu, H.; Song, M.; Wei, S. Exposure to Legacy and Novel Perfluoroalkyl Substance Disturbs the Metabolic Homeostasis in Pregnant Women and Fetuses: A Metabolome-Wide Association Study. *Environ. Int.* **2021**, *156*, 106627.
(64) Liu, Y.; Li, A.; An, Q.; Liu, K.; Zheng, P.; Yin, S.; Liu, W. Prenatal and Postnatal Transfer of Perfluoroalkyl Substances from Mothers to Their Offspring. *Crit. Rev. Environ. Sci. Technol.* **2022**, *52* (14), 2510−2537.
(65) Xia, X.; Zheng, Y.; Tang, X.; Zhao, N.; Wang, B.; Lin, H.; Lin, Y. Nontarget Identification of Novel Per- and Polyfluoroalkyl Substances in Cord Blood Samples. *Environ. Sci. Technol.* **2022**, *56* (23), 17061−17069.
(66) Zhang, B.; Wei, Z.; Gu, C.; Yao, Y.; Xue, J.; Zhu, H.; Kannan, K.; Sun, H.; Zhang, T. First Evidence of Prenatal Exposure to Emerging Poly- and Perfluoroalkyl Substances Associated with E-Waste Dismantling: Chemical Structure-Based Placental Transfer and Health Risks. *Environ. Sci. Technol.* **2022**, *56* (23), 17108−17118.
(67) Fan, Y.; Guo, L.; Wang, R.; Xu, J.; Fang, Y.; Wang, W.; Lv, J.; Tang, W.; Wang, H.; Xu, D.-X.; Tao, L.; Huang, Y. Low Transplacental Transfer of PFASs in the Small-for-Gestational-Age (SGA) New-Borns: Evidence from a Chinese Birth Cohort. *Chemosphere* **2023**, *340*, 139964.
(68) Li, Q. Q.; Huang, J.; Cai, D.; Chou, W. C.; Zeeshan, M.; Chu, C.; Zhou, Y.; Lin, L.; Ma, H. M.; Tang, C.; Kong, M.; Xie, Y.; Dong, G. H.; Zeng, X. W. Prenatal Exposure to Legacy and Alternative Per- and Polyfluoroalkyl Substances and Neuropsychological Development Trajectories over the First 3 Years of Life. *Environ. Sci. Technol.* **2023**, *57* (9), 3746−3757.
(69) Li, X.; Liu, H.; Wan, H.; Li, Y.; Xu, S.; Xiao, H.; Xia, W. Sex-Specific Associations between Legacy and Novel per- and Polyfluoroalkyl Substances and Telomere Length in Newborns in Wuhan, China: Mixture and Single Pollutant Associations. *Sci. Total Environ.* **2023**, *857* (Pt 3), 159676.
(70) He, Y.; Lv, D.; Li, C.; Liu, X.; Liu, W.; Han, W. Human Exposure to F-53B in China and the Evaluation of Its Potential Toxicity: An Overview. *Environ. Int.* **2022**, *161*, 107108.
(71) Lu, Y.; Guan, R.; Zhu, N.; Hao, J.; Peng, H.; He, A.; Zhao, C.; Wang, Y.; Jiang, G. A Critical Review on the Bioaccumulation, Transportation, and Elimination of per- and Polyfluoroalkyl Substances in Human Beings. *Crit. Rev. Environ. Sci. Technol.* **2024**, *54* (2), 95−116.
(72) Cao, H.; Zhou, Z.; Hu, Z.; Wei, C.; Li, J.; Wang, L.; Liu, G.; Zhang, J.; Wang, Y.; Wang, T.; Liang, Y. Effect of Enterohepatic Circulation on the Accumulation of Per- and Polyfluoroalkyl Substances: Evidence from Experimental and Computational Studies. *Environ. Sci. Technol.* **2022**, *56* (5), 3214−3224.
(73) Yi, S.; Yang, D.; Zhu, L.; Mabury, S. A. Significant Reductive Transformation of 6: 2 Chlorinated Polyfluorooctane Ether Sulfonate to Form Hydrogen-Substituted Polyfluorooctane Ether Sulfonate and Their Toxicokinetics in Male Sprague-Dawley Rats. *Environ. Sci. Technol.* **2022**, *56* (10), 6123−6132.
(74) Personne, S.; Brochot, C.; Marcelo, P.; Corona, A.; Desmots, S.; Robidel, F.; Lecomte, A.; Bach, V.; Zeman, F. Evaluation of Placental Transfer and Tissue Distribution of Cis- and Trans-Permethrin in Pregnant Rats and Fetuses Using a Physiological-Based Pharmacokinetic Model. *Front. Pediatr.* **2021**, *9*, 730383.
(75) Ke, A. B.; Milad, M. A. Evaluation of Maternal Drug Exposure Following the Administration of Antenatal Corticosteroids During

Late Pregnancy Using Physiologically-Based Pharmacokinetic Modeling. *Clin. Pharmacol. Ther.* **2019**, *106* (1), 164−173.
(76) Schacht, C. M.; Meade, A. E.; Bernstein, A. S.; Prasad, B.; Schlosser, P. M.; Tran, H. T.; Kapraun, D. F. Evaluating the Impact of Anatomical and Physiological Variability on Human Equivalent Doses Using PBPK Models. *Toxicol. Sci.* **2024**, *200* (2), 241.

https://doi.org/10.1021/acs.est.4c05405
Environ. Sci. Technol. 2024, 58, 18928−18939